International Journal of Pharmaceutics 674 (2025) 125452

Contents lists available at ScienceDirect

International Journal of Pharmaceutics

journal homepage: www.elsevier.com/locate/ijpharm

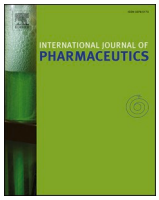

Best practice for the size analysis of nanomedicines – An iron sucrose case study

Ryan T. Coones [a], Ines Nikolic [b,*], Remo Eugster [c], Dora Mehn [d], Vivan Tong [a], Paola Luciani [c,*], Caterina Minelli [a,*]

[a] National Physical Laboratory, Teddington, UK
[b] School of Pharmaceutical Sciences, Faculty of Science, University of Geneva, Geneva, Switzerland
[c] Department of Chemistry, Biochemistry and Pharmaceutical Sciences, University of Bern, Bern, Switzerland
[d] European Commission, Joint Research Centre (JRC), Ispra, Italy

ARTICLE INFO

Keywords:
Iron-sucrose
Nanosimilars
Nanoparticles
Dynamic-light scattering
Interlaboratory comparison study

ABSTRACT

Iron sucrose is used in the parenteral treatment of iron deficiency anaemia. A number of iron sucrose similars have been developed alongside the original product. These products consist of colloidal iron with particles in the nanometre range stabilised by sucrose molecules. Dynamic light scattering (DLS) is the method of choice for the qualification of iron sucrose products in terms of particle size. However, the broad range of instrumentation and accessories available today for the execution of these measurements requires that best laboratory practice is established to ensure measurement comparability and consistent product quality. In this work, we have examined the measurement of iron sucrose particle size by DLS using a range of instrument models and manufacturers and compared results. We performed transmission electron microscopy with cryogenic capability to support DLS data interpretation. We find that DLS results are consistent when equivalent settings are selected across instruments, we discuss the experimental parameters of importance for high-quality measurements and present preliminary data for emerging modalities. Although focussed on iron sucrose products, the outcome of this work is relevant to the analysis of other types of nanoparticle-based products.

1. Introduction

Nanomedicine, the application of nanotechnology in medical science, has delivered step-change innovations in diagnostic procedures, therapy, and prevention of diseases. In the context of drug development, advanced formulations and drug delivery systems have enhanced therapeutic efficacy and targeting, while reducing side effects of active pharmaceutical ingredients (APIs) (Peer et al., 2007). Although the beginning of the nanomedicine era is almost universally associated with the appearance of liposomal doxorubicin formulations, the story of these medicinal products actually began with the iron-based (iron sucrose) nanoparticle formulations as early as 1947 (Nikravesh et al., 2020), which is almost 30 years before the term "nanotechnology" was even coined (Bayda et al., 2020). Since then, a lot of expectation has been placed on drug nanoformulations, and their development has undergone several distinct stages, each characterized by different levels of productivity, technological advancements, and clinical applications (Li et al., 2017).

Among a variety of nanomedicines available on the market today, iron oxide and oxyhydroxide nanoparticles are designed to treat iron-deficiency anaemia and have gained significant attention due to their distinctive physicochemical properties (Nikravesh et al., 2020; Krupnik et al., 2023). A notable applied example of these nanoparticles is iron sucrose, which has seen its formulation evolve over the decades and eventually the emergence of nano-similars. These iron-carbohydrate complexes, designed for parenteral use, offer distinct advantages over oral iron-based preparations including improved bioavailability, reduced gastrointestinal side effects, and faster repletion of iron stores (Krupnik et al., 2024; Auerbach and Ballard, 2010). As of 2024, in Europe there are more than 30 producers of iron sucrose complexes for parenteral administration (Martin-Malo et al., 2019; Rottembourg et al., 2011; European Medicines Agency, 2021).

The structure of iron sucrose has been extensively studied, revealing a complex matrix composed of polynuclear iron(III)-oxyhydroxide nanoparticulate cores stabilized by sucrose molecules (Borchard, 2015; Digigow et al., 2024). For this reason, iron sucrose formulations

* Corresponding authors.
E-mail addresses: ines.nikolic@inoge.ch (I. Nikolic), paola.luciani@unibe.ch (P. Luciani), caterina.minelli@npl.co.uk (C. Minelli).

https://doi.org/10.1016/j.ijpharm.2025.125452
Received 20 December 2024; Received in revised form 6 February 2025; Accepted 7 March 2025
Available online 8 March 2025

are classified as non-biological complex drugs (NBCDs) (Mühlebach and Flühmann, 2015). The unique arrangement of iron and sucrose not only enhances the stability of the formulation but also contributes to its overall safety profile, offering controlled release of iron and ensuring a steady supply of the element for erythropoiesis. The release of iron appears to be influenced by the size and surface properties of the colloidal iron complex and the matrix. However, depending on the manufacturing procedure (which typically consists of numerous steps), available iron sucrose products may differ significantly in the physicochemical aspects, which in turn impacts pharmacological performance and clinical efficacy (Martin-Malo et al., 2019; Rottembourg et al., 2011).

Due to the difficulty to fully characterise and define iron complex-based particles and the uncertainties on how quality attributes relate to *in vivo* performance, it has been recognized that the regulatory evaluation of the therapeutic equivalence of the follow-on products (iron sucrose nano-similars) could not be based on conventional bioequivalence studies alone. Trying to provide clarity in the area of NBCDs, the European Medicines Agency (EMA) published a reflection paper summarizing the data requirements for market authorisation of iron-based nano-colloidal products (European Medicine Agency, 2013). In addition, the U.S. Food and Drug Administration (FDA) has published draft guidance for industry, covering characterisation and directions for bioequivalence testing of three different intravenous iron products, among which is the iron sucrose complex (Food and Drug Administration, 2013; Food and Drug Administration, 2024; Food and Drug Administration, 2012). These documents encompass suggestions for rigorous testing and validation processes to confirm the pharmacokinetics, pharmacodynamics, and therapeutic equivalence of nano-similars to their original counterparts. Documentary standards for quality testing of these products are still under development in Europe and the aim of the presented study is to support these efforts.

Particle size plays a critical role in the efficacy and safety of parenteral drug delivery systems, and it is recognised as one of the critical quality attributes (CQAs) for nanomedicines. In the case of iron sucrose nanoparticles, size directly influences the pharmacokinetics, biodistribution, and cellular uptake of the product. Despite nanoparticle size being outlined as one of the main physicochemical aspects in the regulatory decision-making process, clear and standardised practice for iron sucrose products is lacking (Halamoda-Kenzaoui et al., 2021; European Medical Agency, 2016). Stringent quality control measures are essential to maintain the consistency of product particle size within the desired range. There is no unique method to measure this attribute, but dynamic light scattering (DLS) has become a ubiquitous method which is employed both during development and qualification of complex medicines and is able to provide fast measurements of the particle size distribution (PSD) and stability of the formulation, with minimal sample preparation. However, a number of DLS instrument models are available on the market at present, with differences in settings and performance. The development of universal best practice, quality guidelines and standards for iron sucrose and other complex medicines requires that instrument variability is understood and considered. In this study, we present a comprehensive size analysis of iron sucrose nanoparticles through an interlaboratory comparison of 5 different DLS instrument models, performed at 5 laboratories in Europe. Through this approach, we provide harmonised guidance to future quality standards to measure the size of iron-based nanoparticles by DLS.

Although the insights gained in this study are based on a specific type of nanomedicine, namely iron sucrose, the general conclusions and recommendations are broadly applicable to other complex drugs and nanomedicine products. The authors aim to offer valuable guidelines and measurement best practice for the further development of quality standards for size measurements as one of the main CQAs of nanomedicines.

2. Materials and methods

Four sample batches containing 30 mg/mL iron sucrose were received in collaboration with the European Directorate for the Quality of Medicines & HealthCare (EDQM), referred to as batch 1, batch 2, batch 3, and batch 4 respectively. The iron sucrose batches used in this study were provided by the EDQM and the details of the manufacturer remain confidential. The samples were industrially manufactured according to industrial standards but re-labelled by the EDQM to maintain anonymity. Information on the nature of the sample and the iron sucrose concentration was provided, along with safety data sheets for the compounds. Iron sucrose samples were diluted 1:50 in filter sterile solutions of ultrapure water or 0.9 % sodium chloride solution. Gentle agitation by inverting the vial was applied before dilution and measurements. Samples of each batch of stock solution were distributed initially to each laboratory, and then were freshly prepared by dilution from stock for each measurement session.

Monodisperse polystyrene (PS) spheres of 20 nm nominal diameter (Certified batch 3020–016) applied in quality control measurements were purchased from Thermo Scientific (Waltham, MA, USA) (3000 Series Nanosphere™ Size Standards, Catalogue number 3020 A). The monodisperse PS suspension contained spheres with a mean diameter of (22 ± 2) nm ($k = 2$, i.e. 95 % confidence level) as measured by DLS and was traceable to the spheres certified by the National Institute of Standards and Technology (NIST, Standard Reference Material 1963, 1964 or 1961). The nominal mass concentration of the undiluted standard was 1 % (w/v) (not certified) and spheres were assumed to have a density of 1.05 $g \cdot cm^{-3}$ (Kestens et al., 2017). When diluted, spheres were dispersed in ultrapure water (resistivity of 18.3 MΩ•cm) previously filtered using a 0.2 μm cutoff syringe filter (Merck, Rahway, NJ). A range of cuvettes (see L6 in Table 1), dilutions and instrumental parameters (measurement position and laser attenuator) were tested in order to determine optimal measurement conditions. The tested cuvettes differed in type of material and wall thickness, namely polymethyl methacrylate (PMMA), PS and quartz, where the disposable PS cuvettes had the thinnest walls (0.95 mm), PMMA cuvettes had 1.1 mm thick walls and a quartz cuvette had a wall thickness of about 1.2 mm.

DLS instruments used in this work are listed in Table 1. Instruments at L1 to L5 were used for the interlaboratory comparison on iron sucrose products. All measurements were performed with a sample equilibration time of 120 s, and the procedures were configured to ensure that the SOPs used for measurements in this study comply with the DLS chapter of the European Pharmacopoeia (European Pharmacopoeia, 2024). A total of four samples of iron sucrose were measured. Within-day method variability was evaluated by measuring 6 repeats of 3 aliquots per sample. Between day-variability was evaluated by measuring 6 repeats of 1 aliquot per sample over three days. The instrument at L6 was used to study the impact of measurement settings, including the type of cuvette and the measurement position, on the DLS results.

For transmission electron cryomicroscopy (cryo-TEM), iron sucrose particles from batch 3 were 50 times diluted in water immediately before blotting. Lacey carbon films coated with ultrathin carbon films mounted on Cu 200 mesh grids (Agar Scientific, UK) served as the substrate for sample deposition. Initially, these grids were subjected to plasma cleaning at 230 V and 15 Pa vacuum for a duration of 30 s. Subsequently, a 4 μL aliquot of the diluted sample was pipetted onto the carbon coated side of the prepared grids. For the samples, the blotting chamber was pre-conditioned to a controlled environment of 21 °C and 100 % humidity. The samples were plunge-frozen using a Vitrobot (FEI, Hillsboro, USA). Excess liquid from these samples was automatically blotted away using two strips of filter paper and blot time of 4 s was employed, followed by immediate plunge-freezing into liquid ethane maintained at − 180 °C. The prepared grids were then stored in liquid nitrogen until they were ready for microscopy. Low-dose electron diffraction studies were carried out using a FEI Tecnai Spirit F20 electron microscope. Imaging was performed at an acceleration voltage of

Table 1
List of DLS instruments assessed in this work and the corresponding measurement settings.

Lab. #	Instrument model	Instrument manufacturer	Laser source wavelength and power	Software	Scattering angle (air)	Cuvettes
L1	Zetasizer Ultra	Malvern Panalytical (Malvern, UK)	633 nm < 10 mW	Zetasizer ZS Xplorer v. 3.2.1.11	173° (DLS) 17°, 90°, 173° (MADLS)	Disposable polystyrene, DTS0012
L2	Litesizer 500	Anton Paar (Graz, Austria)	658 nm 40 mW	Kalliope Ink V: 2.30.4	175°	Disposable PMMA, Sarstedt 67.740
L3	Zetasizer Nano ZS	Malvern Panalytical (Malvern, UK)	633 nm < 10 mW	Zetasizer Nano 0v.7.13	173°	Disposable polystyrene, DTS0012
L4	Zetasizer Nano ZS	Malvern Panalytical (Malvern, UK)	633 nm < 10 mW	Zetasizer Nano 0v.7.5	90°	Disposable polystyrene, DTS0012
L5	Amerigo	Cordouan Technologies (Pessac, France)	638 nm < 50 mW	AmeriQ_x64	170°	Disposable polystyrene cuvettes 7,697,101
L6	Zetasizer Nano ZS	Malvern Panalytical (Malvern, UK)	633 nm < 10 mW	Zetasizer Nano 0v.7.12	173°	Non disposable Quartz; Disposable PMMA BRAND BR759115; Disposable polystyrene, Sarstedt 67.754

80 kV, and the captured images were recorded using an FEI Eagle CCD Camera.

3. Results

3.1. Considerations on DLS experimental conditions

DLS instrument performance prior to measurement of the iron sucrose was assessed with a polystyrene sphere dispersion with a certified value for the hydrodynamic diameter as measured by the manufacturer with DLS. The choice of a range of experimental and instrumental parameters was assessed. Fig. 1(a) and 1(b) illustrate the impact of the measurement position on the resulting particle Z-average and polydispersity index (PDI) respectively as a function of cuvette type, namely made of PMMA, PS and quartz. For clarity, Fig. S1 shows the relative position value of each of the model set-ups with respect to the

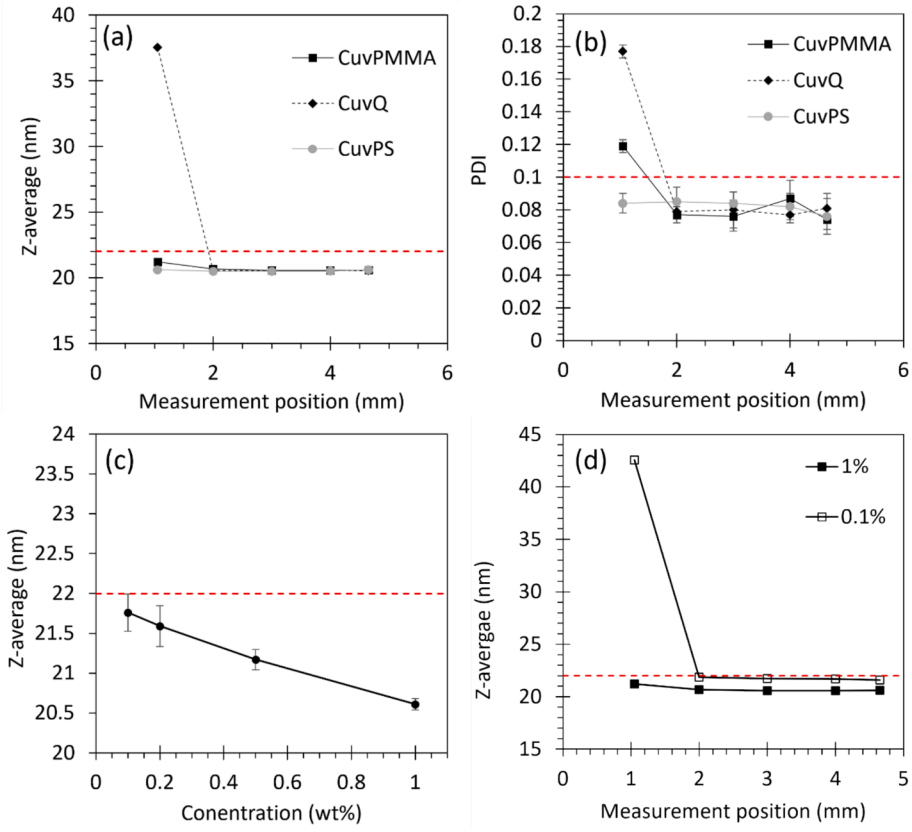

Fig. 1. Measured (a) Z-average and (b) PDI values as a function of the measurement position of 1 % w/v dispersions of PS spheres for different cuvette material types (PMMA cuvettes – black squares; Quartz cuvettes – black diamonds; Polystyrene cuvettes – grey circles). (c) The effect of the dispersion concentration on the measured Z-average value, and (d) effect of measurement position at two different concentrations in PMMA cuvettes.

middle of the cuvette. In the Malvern and Amerigo instruments, a position of 0 mm refers to a measurement hypothetically performed at the outer edge of the cuvette at the air-cuvette interface closest to the laser source, while the centre of the cuvette is closer to position 4.65 mm. For the Anton Paar instrument, a measurement position of 0 mm refers to a measurement taking place at the centre of the cuvette (Table 2). The measurements of the polystyrene particles described in this section were performed with a Malvern instrument. For all cuvette types, Z-average and PDI values were higher at position 1.05 mm than closer to the centre of the cuvette. The disparity in Z-average and PDI suggests that the proximity of the measurement position to the cuvette wall impacts the outcome of the measurement, and the error is more pronounced for the quartz cuvette, which has thicker walls, with respect to the PS cuvette.

Instrument qualification protocols require to perform measurements at specific concentrations. Undiluted samples are straightforward to measure, but experimental parameters may require optimisation where the concentration deviates significantly from the ideal value. The effect of particle concentration was first tested at a fixed attenuator value of 5 (0.1 % transmission), in PS cuvettes at the 4.65 mm measurement position. The 1 % concentration standard was measured undiluted and at dilutions of 2x, 5x, and 10x, with Fig. 1(c) showing that the measured Z-average values decreased with increasing concentration of the standard. This result suggests that the undiluted dispersion was not optimal for DLS measurements, with multiple light scattering and/or particle interaction likely occurring (International Organization for Standardization, 2017). At 10x dilution (0.1 % w/v) the measured Z-average value was closer to the expected certified value.

The comparison between the original and 10x diluted PS standard at various measurement positions (Fig. 1(d)) was next run in PMMA cuvettes at a fixed attenuator value of 5. In the case of the 0.1 % w/v dispersion, the measurement position 1.05 mm provided a Z-average result of 42.6 nm – clearly outside the expected range. In contrast, the more concentrated dispersion gave Z-average values closer to the expected value at the same position. The PDI values for both suspensions were, however, outside the acceptance limit at this position. On the other hand, PDI values for both suspensions were found to be < 0.1 at measurement points closer to the centre of the cuvette (i.e. $\approx$4.6 mm). Z-average values were found to be closer to the expected 22 nm in the case of the 0.1 % dispersion with respect to the 1 % dispersion at all positions other than the 1.05 mm.

The measurement position automatically selected by the software is 4.65 mm (close to the centre of the cuvette). The automatically selected attenuator values at this position are 6 and 8 for the 1 % w/v and 0.1 % w/v dispersions respectively. The best match between the expected mean size value and measured Z-average while maintaining low measurement variability was observed for the 0.1 % w/v dispersion using automatic measurement position and automatic attenuator selection. Furthermore, the total measurement duration for 6 repeated measurements of the 0.1 % w/v dispersion and fixed attenuator value 5 was about 60 min, while with automatic attenuator value 8 the 6 measurements requested about 12 min.

3.2. Iron sucrose measurement by cryo-TEM

Fig. 2(a) and 2(b) show representative cryo-TEM micrographs of iron sucrose where a rod-like structure is observed. Fig. 2(c) and (d) show darker areas of higher electron density where there is apparent aggregation of the iron sucrose around regions of suspected sucrose. Representative negative staining TEM micrographs of the iron sucrose product are shown in Fig. S2. The sample confirms the presence of particles with rod-like structures. By increasing magnification, it was revealed that these rod-like structures are multicomponent, and not single iron-based particles.

3.3. DLS measurement of iron sucrose

DLS measurements of iron sucrose were carried out in the different laboratories according to the parameters outlined in Table 2. In all cases, the instrumental settings for measuring the iron sucrose were automatically chosen by the instrument software. However, a requirement for measurement repeats was set so that the number of “measurements runs” (30 to 60) and their “duration” (10 s) was comparable across the instruments.

The results of the iron sucrose DLS measurements performed at the different laboratories are summarised in Fig. 3 and Table S1. Fig. 3(a) shows the scattered-light intensity-based particle size distribution for a representative batch of iron sucrose (batch 1) measured by each laboratory. All distributions exhibited an intense peak around 12 nm. According to the cumulant analysis, the average Z-average and PDI values across all batches and laboratories were (11.8 $\pm$ 0.2) nm and 0.200 $\pm$ 0.016 respectively. We note that for some batches, some of the measured scattered-light intensity-based size distributions exhibited an apparent shallow peak at larger sizes. This peak is not visible in the volume-based or number-based size distributions. The PSD for L5 are omitted from Fig. 3(a) due to the instrument software not allowing numerical export of the data from a measurement, and only a portable document format file can be obtained. Fig. 3(b) and 3(c) show the average Z-average and PDI values of batch 2 measured at the different laboratories. The error bars represent the total variability of both the within-day and between-day variability, calculated as the square root of the sum of the squares of the within- and between-day standard deviations. Table 3 shows the within-day and between-day variability for all batches. Whilst measurement variability varies substantially between the laboratories and, therefore, the instrument models used in the study, the average measured values for the Z-average and the PDI agree within 14 % and 21 % respectively. We note that the Z-average value is affected by the presence of the peak in the large size range and that this was not observed consistently across all the measurement repeats. As a result, this inconsistency increases measurement variability. Representative PSDs from each laboratory for each of the iron sucrose batches are given in Fig. S3. When compared to the dimensions of the needle-like iron sucrose particles observed in Fig. 2, the measured size should be interpreted as the hydrodynamic diameter of the solid sphere with equivalent diffusion coefficient. It should be noted that the DLS instrument utilised

Table 2
Experimental parameters for the measurement of iron sucrose batches.

Experimental Setting	L1	L2	L3	L4	L5
RI water	1.330	1.330	1.330	1.330	1.330
RI saline	1.330	1.332	1.331	1.331	1.331
Temperature (°C)	25 $\pm$ 1	25 $\pm$ 1	25 $\pm$ 1	25 $\pm$ 1	25 $\pm$ 1
Viscosity water (mPa.s)	0.8872	0.8903	0.8872	0.8872	0.8872
Measurement mode	Automatic	Automatic	Automatic	Automatic	Automatic
Attenuator	9	n/a	10	10	10
Optical density filter	n/a	1.44 $\pm$ 0.06	n/a	n/a	n/a
Transmission (% nominal)	10	n/a	30	30	30
Position (mm)*	4.64	−3.62 $\pm$ 0.13	3.00	3.00	3.00

* Refer to Fig. S1 for an illustration of the measurement position with respect to the cuvette geometry for the different instrument models.

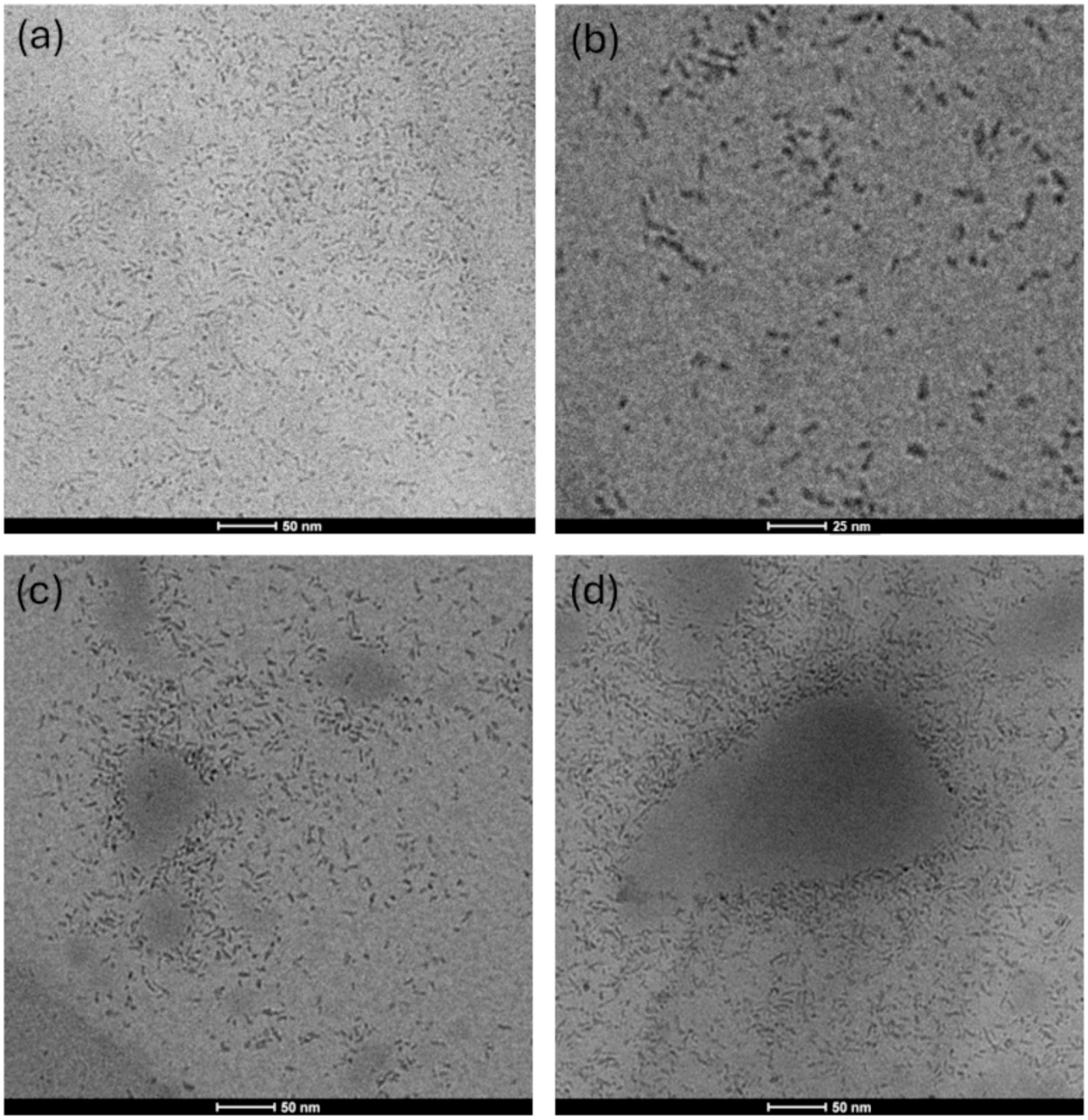

Fig. 2. Cryo-TEM measurements of iron sucrose particles from batch 3. (a) Free particles with a rod-like morphology (b) Free particles at high magnification (c) Mild aggregates of iron sucrose particles around an electron dense structure. (d) Large aggregates surrounded by iron sucrose particles.

in laboratory L4 has a 90° configuration, while the other laboratories utilise instruments with a backscattered configuration. Fig. S4 show that the same measurements performed on iron sucrose samples dispersed in saline solution yield similar results.

Fig. 3(d) and 3(e) show the average Z-average and PDI values respectively measured in a backscattered configuration across the laboratories for each iron sucrose batch. Error bars for the Z-average and PDI values represent the standard deviation of the mean, with average relative values of 7 % and 9 % respectively.

The size distributions of the iron sucrose samples revealed, in some cases, the presence of a peak at a larger size range. To investigate whether this is a real particle population, for example caused by a small number of large sucrose agglomerates, we measured the iron sucrose samples using a DLS instrument collecting the light scattered by the particles at different angles. In Fig. 3 and Table S1 we already presented measurement results from instruments with both backscattered and orthogonal configuration, with no significant difference observed. To further investigate, we utilised the instrument available at Laboratory L1 in multi-angle DLS (MADLS) modality, which is capable of performing measurements at scattering angles in air of 17° (forward scattering), as well as 90° (orthogonal scattering) and 173° (back scattering). We also investigated the effect of a different analytical model on the measured size distribution.

Fig. 4(a) shows the size distributions of one batch of iron sucrose as measured by traditional DLS in backscattering configuration, exhibiting the presence of a particle population at larger size range with respect to the main population. The use of a “multiple narrow mode” algorithm as opposed to the “general purpose” algorithm still suggests the presence of the larger population, although in a lower size range. Fig. 4(b) and 4(c) show the size distributions and related correlograms respectively as

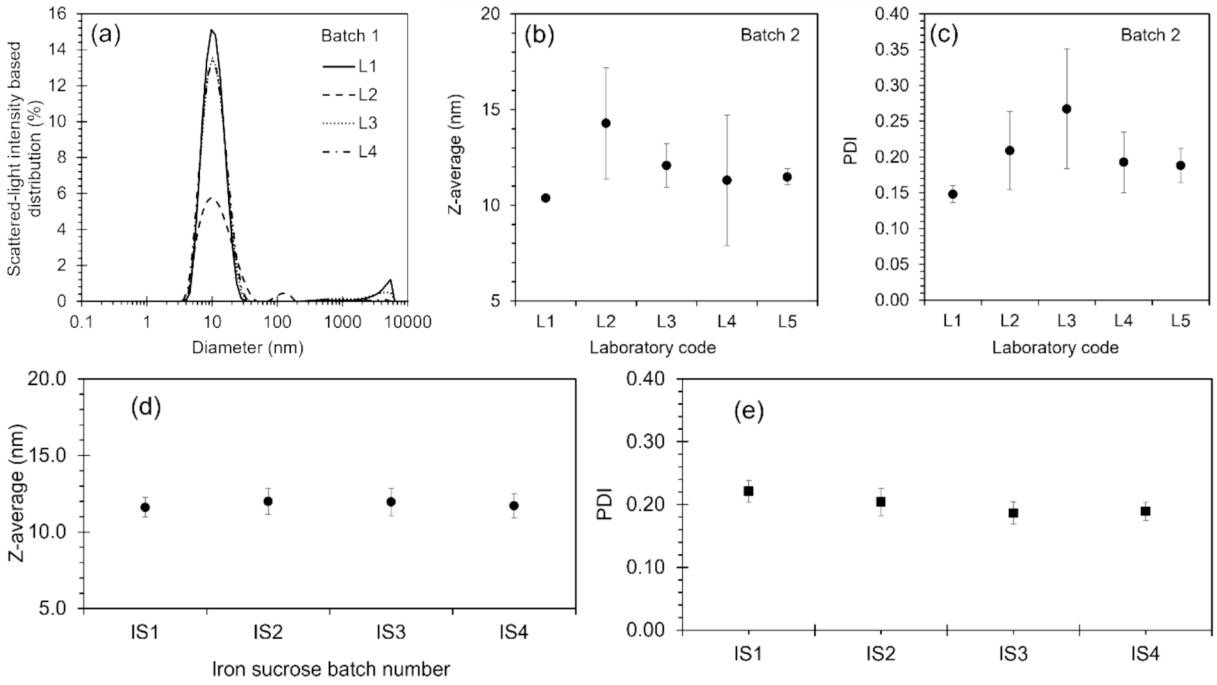

Fig. 3. (a) Representative scattered-light intensity-based particle size distributions of batch 1 of iron sucrose as measured in each laboratory. Average (b) Z-average and (c) PDI values of iron sucrose batch 2 as measured at the different laboratories. (d) Z-average and (e) PDI of the four iron sucrose batches resulting from the average of the measurements performed at the 5 laboratories which performed DLS. Error bars represent the resulting standard error.

Table 3
Average within-day and between-day method variability for the measurement of the Z-average and PDI of four iron sucrose samples diluted in water as measured by DLS.

	Z-average		PDI	
Laboratory	Within-day	Between-day	Within-day	Between-day
L1	1.4 %	0.63 %	12 %	4.1 %
L2	12 %	8.8 %	11 %	9.8 %
L3	6.7 %	5.2 %	25 %	15.4 %
L4	1.4 %	3.2 %	6.9 %	13.5 %
L5	13.5 %	12.3 %	14.5 %	12.3 %

measured at different angles. As previously observed, the measurements performed in backscattered and orthogonal configurations both show minor particle populations at a large size range, although not identical in size. The size distribution resulting from the measurement in forward scattering configuration, however, reveals the presence of a large population at ≈700 nm. When information from measurements at all angles are combined in Fig. 4(d), MADLS indicates the presence of a secondary particle population in the size range between 50 nm and 100 nm.

4. Discussion

4.1. The regulatory and standardisation landscape

The variety of proposed nanomedicine products is posing an analytical challenge because it is recognised that measurement methods require tailoring to the specific nature of the products and no one-size-fits-all analytical solution exist. This challenge has been acknowledged by the regulatory community and has driven the activities of bodies such as the EDQM, EMA and the FDA to provide guidance and standards for specific products. Intravenous iron sucrose has a complex nanoparticle structure typically consisting of a polynuclear iron(III)-hydroxide core surrounded by a large number of non-covalently bound sucrose molecules. The complex has an average molecular weight of approximately 43 kDa. The polynuclear iron core is designed to mimic that of the core of the physiological iron storage protein ferritin and to provide iron transferrin and ferritin proteins in a controlled way (Funk et al., 2022; Kontoghiorghes et al., 1987; Le Brun et al., 1800). Based on the EM micrographs, the morphology of the iron sucrose complexes could be described as rod–like. Most likely, these elongated structures represent clusters of multiple iron nanoparticles in the dense sucrose envelope, and not single iron sucrose particles. These assumptions are consistent with recently published data by Krupnik et al. (2023) where using small angle X-ray scattering (SAXS) a structural model of iron sucrose was proposed, reported as an elongated structure composed of multiple iron sucrose particles, while the degree of agglomeration was dependent on the dilution.

The measurement of hydrodynamic size of these particles is one of the CQAs that is typically measured for product characterisation and qualification. The need for harmonisation and standardisation in the characterisation of nanomedicines, and in particular with respect to their CQAs, has become increasingly evident (Di Francesco et al., 2019; Astier et al., 2017; Clogston et al., 2020). Specifically, there is a need for best practice and standardised measurement protocols that are tailored to the specific nanomedicine product and analytical method, while at the same time overarching across varying instrument models, manufacturers, and differing accessories. This need is highlighted by the variability shown in the results section, in particular, in Fig. 3 where variation is shown across measurements of iron sucrose on different instruments and batches of iron sucrose. For product qualification, operating procedures need to be sufficiently detailed to enable measurement comparability and consistent result interpretation, whilst remaining brand agnostic.

In this work, we compared the performance of 5 different DLS instrument models for the measurement of the hydrodynamic size of iron sucrose. DLS is a robust and ubiquitous method for particle sizing in both research and quality control environments. DLS has been the subject of standardisation within the international community, with documentary standards, technical reports, and best practices available from the International Organization for Standardization (ISO) (ISO 22412:2017, ISO/TR 22814:2020), ASTM international (ASTM E3247-20), scientific bodies (US National Cancer Institute), along with additional compendial

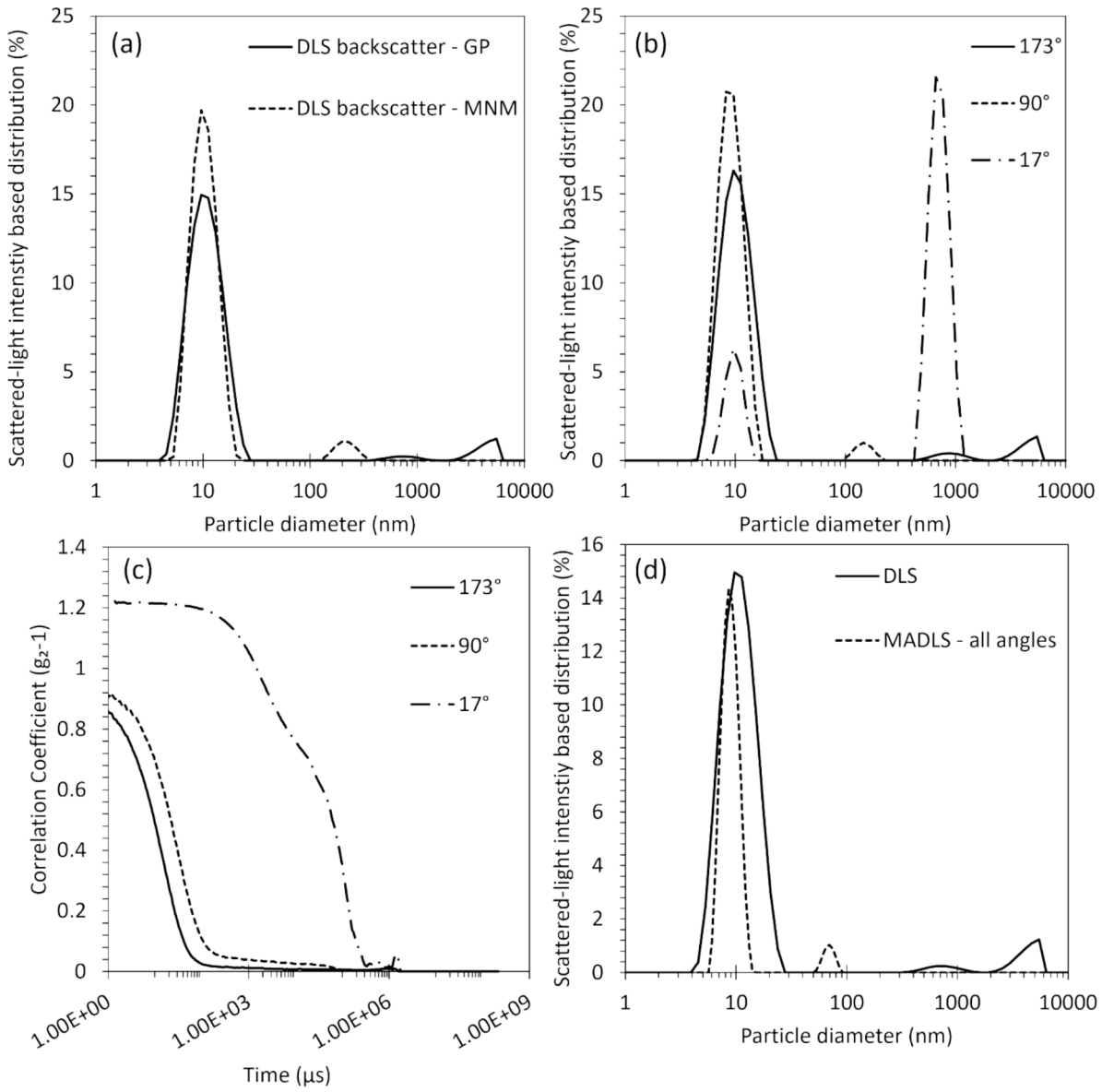

Fig. 4. (a) Scattered-light intensity-based size distributions of iron sucrose batch 1 measured by DLS using both general purpose (GP) (solid line) and multiple-narrow-mode (MNM) (dashed line) analysis modes. (b) The PSDs for scattering angles in air of 173° (solid line), 90° (dashed line), and 17° (dot + dashed line) as measured by MADLS along with (c) the corresponding correlograms of MADLS measurement at detector angles of 173° (solid line), 90° (dashed line), and 17° (dot + dashed line). (d) A comparison of scattered-light intensity-based particle size distributions as measured by DLS (solid line) and MADLS (dot + dashed line).

requirements (Hackley et al., 2010; International Organization for Standardization, 2020; International Organization for Standardization, 2017; European Pharmacopoeia, 2024). For clarity of comparison, Table 4 gives a summary of each of the procedure or standards cited above in terms of their scope, and their guidance on instrumentation, sample preparation, measurement parameters, validation, and data analysis. We note, however, that there is no specific guidance on the application of the DLS method to iron sucrose products and this work directly addresses this gap by discussing the results of an interlaboratory comparison performed by using 5 different DLS instrument models available at different laboratories across Europe cooperating under the umbrella of the EDQM.

DLS instrumentation measures the translational diffusion of nanoparticles that are moving under Brownian motion, estimating the hydrodynamic diameter by monitoring changes in the intensity of the light scattered by the sample as a function of time (hereafter referred to as the autocorrelation function), where the viscosity and temperature of the dispersant solution are accurately known (International Organization for Standardization, 2017). In order to extract the particle diameter from the autocorrelation function two main methods are commonly used. For monomodal particle distributions, the cumulant method expands the measured autocorrelation function into a second-order power series, where the Z-average (intensity-weighted harmonic mean hydrodynamic diameter) and polydispersity index (PDI) are the first and second terms of the power series respectively (International Organization for Standardization, 2017). Non-negative least squares algorithms (NNLS), among other methods, are used to output a scattered-light intensity-weighted particle size distribution (Farkas and Kramar, 2021). By applying knowledge of the optical properties of both the dispersant and the nanoparticles the intensity-weighted particle size distributions can be transformed into volume and number-based distributions (Bloomfield, 1985).

4.2. *Assessment of instrument performance using reference size standards*

Quality control materials are routinely used to assess the

Table 4
Summary of guidance provided by the DLS standards in Ph. Eur. (monograph 2.9.50), ASTM E3247-20, ISO 22412:2017, and NIST-NCL/EUNC PCC1 protocol.

Constituent part	Ph. Eur. 11 (monograph 2.9.50)	ASTM E3247-20	ISO 22412:2017	NIST-NCL/EUNC PCC1 protocol
Scope	General procedure for the application of DLS to pharmaceutical products, with a focus on quality control.	General procedure for the measurement of nanoparticle size using batch-mode (off-line) DLS in aqueous suspensions that is applicable to many commercial DLS instruments.	General procedure for the application of DLS to the measurement of particle size and size distribution of mainly submicrometer sized particles, emulsions or fine bubbles dispersed in liquid.	Procedure for the application of DLS specifically related to preclinical characterisation of nanoparticles intended for medical application
Instrumentation	An instrument with a coherent laser source, an optical setup that can focus and direct the beam to a detector at a fixed angle. The sample environment should be capable of temperature control. The PC and software should be able to control the instrument during measurement and analyse the data collected.	DLS instrument operating at single or multiple angles and including a coherent laser ‘ laser beam and to detect scattered photons over very short time intervals, a sample chamber capable of maintaining constant temperature, a photodetector, a correlator and a PC with control software to perform measurements and to analyse data. DLS instruments that use substantially different measurement principles or optical configurations are out of scope.	DLS instrument consisting of a coherent laser source, optical equipment that focuses light, directs the light to a detector for detecting scattering. Hardware capable of obtaining particle size as an output are also required. The sample environment should be temperature controlled.	Any suitable DLS instrument with batch measurement capability.
Sample Preparation	Test samples should be dispersed in liquid that does not absorb at the laser wavelength. The dispersant should be free of contaminants and must not interfere with the test sample chemistry. The sample concentration must be within an “appropriate range”.	Samples must be measured at an appropriate concentration in a clean cuvette. Samples should be handled in such a way that particulate contamination is prevented.	Preparation of samples must ensure proper sample dispersion, avoidance of aggregation, and use of appropriate diluents. A scattering intensity of the sample is recommended to be 10x greater than that of the diluent. Test samples should be given sufficient time to reach thermal equilibrium with the desired measurement temperature in the sample holder.	Sample must be handled with care, taking into consideration all relevant parameters that could influence the results, including sample concentration, absorbance, dust contamination, salt concentration, pH.
Measurement parameters	The refractive index of the sample should be known to be different from the dispersant. The viscosity of the dispersant, and measurement temperature are also required. The results must include an average particle diameter and polydispersity.	Input of the correct refractive index, absorption, and viscosity of the suspending medium is required, as well as the sample temperature.	Refractive index, absorption, and viscosity values of the dispersant are required, as well as the temperature of the measurement.	Refractive index, absorption, and viscosity values of the dispersant are required, as well as the temperature of the measurement.
Validation	Instrument must be checked after it is first installed, if abnormal performance is suspected and yearly with certified reference materials with appropriate average particle size verified by DLS or TEM.	Reference materials or quality control materials should be measured routinely to ensure correct instrument behaviour. Additionally, validation of the sample preparation method should be demonstrated.	Measurement of CRMs with values for DLS should be used to check instrument performance is within range. CRMs should be selected to match the sample chemistry and morphology as closely as possible.	Instrument verification must be performed using an appropriate quality control standard (CRMs).
Data Analysis	Details of the analysis program must be specified in the report, but no guidance or constraints are provided *per se*.	Detailed descriptions of data analyses are not included, although further documentation is cited; however, the average hydrodynamic diameter should be reported along with the polydispersity index. Further, the results of the cumulants analysis should always be reported irrespective of the analysis model used.	Various analysis models (cumulants, NNLS, CONTIN, etc.) are available for the evaluation of measurement results. The choice of algorithm should be reported along with any other internal settings when reporting DLS data.	The document focuses on cumulant analysis, but detailed descriptions of data analysis are not provided.

performance of an instrument or a method and demonstrate they are fit-for-purpose. For example, the European Pharmacopeia foresees the quality control of the instrument applied for DLS measurements using reference materials with “appropriate” average size verified by DLS or electron microscopy (European Pharmacopoeia, 2024). The relevant ISO standard (22412:2017) recommends the use of certified standards with reference values generated using the same evaluation algorithm or – as an alternative – certified polystyrene standards with average size determined by DLS or electron microscopy (International Organization for Standardization, 2017). It is best measurement practice to perform the quality control measurements using a size standard similar in size to the tested product and preferably certified with the same method. As seen in the results section, iron sucrose formulations include particles with average hydrodynamic diameter of around ≈12 nm and whose size distribution approaches the lower limit of the working range of typical DLS instruments. In this size range, proper particle standard selection becomes challenging, as hydrodynamic diameter might significantly deviate from the size determined by EM, because of the electric double layer or if particles are stabilised by a surface coating that is not electron-dense enough to be observed by EM (as in the case of some PEG-coated gold nanoparticles) (Maguire et al., 2018; International Organization for Standardization, 2017). For this reason, a monodisperse PS sphere suspension with certified particle mean hydrodynamic diameter of (22 ± 2) nm (k = 2) was selected as the quality control standard. PS spheres are

often materials of choice for qualification purposes because they tend to be stable and can be manufactured with well-defined spherical geometry and narrow size distributions. In the context of DLS, PS spheres are efficient light-scatterers and they do not absorb at the wavelength typically applied in these instruments.

We used this material to investigate the impact of experimental parameters including particle concentration, measurement position, i.e. the point inside the cuvette where the laser is focused and the measurement occurs, and cuvette type on the DLS measurement outcome, to raise awareness on the need for comprehensive and detailed operating procedures to ensure measurement comparability. Controlling particle concentration is important to ensure the particles move under pure Brownian motion, thus fulfilling the assumption underpinning the DLS method. If particles are too concentrated, the likelihood of a scattered photon being re-scattered by neighbouring particles increases, leading to an apparent decrease in the particle size, as seen in Fig. 1(c) (Ragheb and Nobbmann, 2020). For instruments in backscattering configuration, measurements performed at the edge of a cuvette, as opposed to the centre, afford higher concentrations of the dispersions (Malvern Panalytical, 2014). Performing the measurement at the edge of the cuvette rather than the centre allows accurate determination of instrument performance using the undiluted size standard (1 % w/v). However, this setup also increases the possibility of flaring, that is the reflection of a portion of the incident light beam into the detection optical path, which typically manifests as spurious peaks in the $>$ 1 μm size region. Boundary effects at the cuvette-liquid interface are also possible, which change the particle diffusion behaviour at the cuvette-liquid interface with respect to the particles in bulk solution (Uhlmann et al., 1964). Fig. 1(a) and 1(b) show that cuvettes made of different materials, and having different wall thicknesses, impact differently the measurement of the particle Z-average and PDI at positions close to the edge of the cuvette. In fact, only the measurements performed with PS cuvettes, which have the thinnest walls, afford results consistent with the particle certification and/or performance requirements (PDI $\leq$ 0.1). As the concentration of the particle dispersion decreased, inaccuracies of measurements performed at the edge of the cuvette increased (Fig. 1 (d)).

For quality purposes and where brief measurement times and straightforward procedures are important, performing measurements of undiluted samples at typical concentrations of 1 % w/v may be of advantage. We note that even if these concentrations may not output the measurement results closest to the certified values of the quality test material, they are still within the certified uncertainty, provided that the cuvette type and measurement positions are correctly selected. However, in case of this particle standard, 10x dilution of the original suspension resulted in Z-average values closer to the expected mean size (even in a thicker, PMMA cuvette) when measured at the centre of the cuvette and for this reason a dilution factor 10 is recommended when measuring this material. We also note that for both 0.1 % w/v and 1 % w/v concentrations, the measurement results obtained when letting the instrument auto-select the optimal measurement position and attenuator are in better agreement with the certified value, with respect to results obtained from selecting a manual measurement position. These results confirm that detailed and standardised operating procedures are required to enable measurement comparability and consistent instrument and product qualifications.

For accurate DLS results, the sample concentration needs optimisation to avoid on one hand the occurrence of multiple scattering and particle–particle interactions at high concentration regimes, and on the other hand sample instabilities and agglomeration due to excessive dilution. This requirement needs to be balanced with a suitable signal-to-noise ratio enabling the required measurement precision, which depends on the nature of the sample and its ability to scatter light efficiently. It is best practice to perform DLS measurements on a series of dilutions to identify optimal concentration (International Organization for Standardization, 2017). Our investigation of 30 mg/mL iron sucrose samples indicated a 50x dilution as optimal for DLS measurements across different instrumentations.

4.3. Interlaboratory comparison

We also investigated the stability of the samples in both water and saline solution (Fig. S4) and concluded measurement outcome is similar as long as dispersions are measured within 2 h from the dilution. In this work we present comparative data of measurements performed in ultrapure water and Fig. 3 shows the result of the interlaboratory comparison. Measurement protocols were harmonised so that all laboratories measured a 0.6 mg/mL dispersion of the original sample in ultrapure water, with measurement position selected automatically. The number of "measurements runs" and their "duration" was adjusted manually so to be comparable across the instruments (e.g. 30 runs of 10 s each). However, the instruments were left to select automatically the parameters regulating the amount of light reaching the detectors (named for example "attenuator" or "(optical density) filter" depending on the instrument model). This is in part due to the fact that the different instruments operate with lasers with different wavelengths and powers.

Considering the results from all laboratories employing instruments in backscattering configuration, the average hydrodynamic diameter (expressed as Z-average) of the iron sucrose particles as measured across 4 batches resulted in (11.8 $\pm$ 0.2) nm (i.e. 2 % relative standard deviation (RSD)). The average PDI resulted in 0.200 $\pm$ 0.016 (8 % RDS). The average measurement agreement across the laboratories was 7 % and 9 % for the Z-average and the PDI respectively. For a hydrodynamic diameter of ≈12 nm, this translates to an average measurement reproducibility of 1.6 nm (k = 2), which is close to typical DLS instrument performance. We also note that the instrument operating at 90° at laboratory L4 also produced results within the same level of agreement, confirming the robustness of the measurements, and indicating comparability between measurements acquired in orthogonal and backscattered configurations.

4.4. Reconciling DLS diameter in light of non-spherical cryo-TEM geometry

To interpret the DLS results, the geometry of the particles needs to be taken into account. We observed in Fig. 2 that the iron sucrose particles are not spherical. In such cases, both the translational and rotational diffusion coefficients contribute to the observed hydrodynamic diameters of the particles. The instrument measures the hydrodynamic diameter of the sphere with equivalent diffusion coefficient as the particles in the sample. The cryo-TEM micrographs show the planar projection of the rods, which should be imagined as having, in the three-dimensional space, a range of directions of their elongation axis with respect to the direction perpendicular to the plain. As a result, the maximum rod projection length, ≈12 nm, is interpreted as the rod length, while the minimum rod projection length, ≈4 nm, is interpreted as the rod width (Fig. S5). Using a model for rod-shaped particles proposed by Tirado et al., (Tirado et al., 1984; Hoover and Murphy, 2020) these dimensions result in an equivalent spherical diameter of ≈8 nm. Considering the approximation of the model and the presence of additional sucrose and solvent molecules at the particle surface, and therefore in the hydrodynamic volume of the particles, this result is in good agreement with the Z-average results from DLS measurements, ≈12 nm. The offset in results between the two methods is accounted for in the difference of the measurands between DLS and microscopies where DLS is measuring the hydrodynamic diameter and Z-average is the intensity based harmonic mean, while microscopies measure the projection of electron dense structures that does not include the hydration layer and provide number-based size distribution results. To this point, we emphasise that a larger value for the DLS particle size result is expected.

Robust characterisation of nanomedicines requires validation of methods for assessing CQAs with orthogonal, independent, approaches.

In the case of iron sucrose, we show that the inclusion of techniques such as cryo-TEM improved understanding of the physical properties of the product and aided data interpretation of liquid methods such as DLS (Digigow et al., 2024; Geiss et al., 2025; Mahmoudi, 2021; European Commission, 2023).

4.5. Measurement variability

We observed significant variability in measurement precision, including intermediate (e.g. between-day) precision across instruments (Fig. 3 and Table 3). This variability may depend in part on the instrument model, but instrument age and maintenance routine are also expected to affect the general instrument performance. From this study, L1, L3, and L4 all used the same instrument manufacturer (where L3 and L4 are the same instrument model) and displayed lower variability for Z-averave than for PDI values. By contrast L2 ad L5 had a similar variability for Z-average and PDI values. At the level of a single laboratory, measuring instrument variability is useful to establish both customised instrument qualification criteria and monitoring changes in instrument performance over time. Measurement repeatability is typically the criterion of concern in compendial procedures and relative standard deviations (RSDs) below 10 % are generally considered a benchmark for acceptable performance (U.S. Pharmacopeial Convention, 2017). The presence of the secondary peak in the larger size range which was not consistently measured across measurement repeats was a contributing factor to lower measurement repeatability. In this respect, laboratories should consider whether the iron sucrose samples are sufficiently homogeneous to test instrument repeatability and whether test samples with similar properties, but better homogeneity are available. More generally, it is important to acknowledge the different level of precision across instruments when drafting guidance documentation and standards for product assessment and qualification. It ensures that the inherent differences in precision are accounted for, which improves consistency of measurement results, ultimately leading to more robust and universally applicable regulatory standards and improved confidence in the data generated from different instruments/laboratories.

4.6. Interpretation of DLS PSDs using agglomeration information provided by cryo-TEM

The intensity of the peaks observed in the larger size range suggests these may be due to a very low level of agglomerates present in the sample. It is not possible however to determine from DLS measurements the nature of such agglomerates, for example whether these are caused by sucrose, or iron particles, or a mixture of the two. Furthermore, the formation of agglomerates may be attributed to the dilution effect, which leads to a decrease in sucrose concentration and, consequently, a loss of stabilization. However, based on the cryo-TEM micrographs one could assume that these peaks originate from the presence of bigger particle clusters – that is apparent aggregation of the iron particles around regions of sucrose – or possibly result from cluster-cluster interactions (Krupnik et al., 2024).

We employed MADLS to gather further insights into the potential presence of particle populations at large size ranges (Fig. 4). The use of MADLS is becoming increasingly common as more instruments are being released onto the market with this capability. However, as of yet, no certified reference materials exist for the MADLS technique, which hinders its uptake for quality purposes. There is a large body of work that reports the dependence of the measured particle size distributions on the scattering angles at which DLS instruments perform the measurements (Bryant and Thomas, 1995; Bryant et al., 1996; Cummins and Staples, 1987; Takahashi et al., 2019). By combining measurement data from multiple angles, a particle size distribution with reduced bias of a few large particles on the overall size distribution can be obtained, (Naiim et al., 2015; Al-Khafaji et al., 2020; Sharma et al., 2023). Further, the combination of multiple scattering angles allows improved resolution on samples containing multiple size populations. No significant difference was observed between measurements performed at a 90° angle versus backscattered configurations, except for a reduction in size of the secondary larger particle population in the former. Measurements performed at forward scattering angle, however, revealed the presence of a large population at a larger size range. It is not good practice, however, to consider measurements at this low scattering angle in isolation, as a small number of large particles biases the results in favour of the larger particles. DLS measurements at forward scattering angles also tend to exhibit higher variability than those performed at larger (more backscattered) angles. Instead, measurements at forward scattering angles should be used in combination with those at other scattering angles to improve the overall quality and fidelity of the measured size distribution. The combination of angles is shown in Fig. 4(d) as a MADLS measurement, alongside results from traditional DLS, both in backscattering (or backscattering equivalent for MADLS) configuration. Both modalities agree on the presence of a minor population at a larger size range, with MADLS indicating this range is between 50 nm and 100 nm. This size range is consistent with the high-density clusters observed in the cryo-TEM micrographs in Fig. 2(c) and (d). This population becomes negligible when the size distribution is represented as a volume-based or number-based distribution, as opposed to a scattered-light intensity-based distribution (Fig. S6).

5. Conclusions

In conclusion, we have performed an interlaboratory comparison of the measurement of the hydrodynamic size of iron sucrose particles by DLS as a case study to discuss particle size measurements of nanomedicine products. We purposely utilised instrumentation from different manufacturers or of different models to enable an unbiased and overarching discussion of measurement comparability and associated best practice. Below are the recommendations emerging from our work:

- Measurement comparability, across experiments performed at different moments in time and/or at different locations, requires detailed operating procedures covering type of cuvette and measurement position within it, along with consistent sample preparation details in terms of dispersant, concentration, and time between measurements and preparation. Satisfying these requirements improve measurement reproducibility.
- Instrument precision varies across instruments and may change in time. Systematic evaluation of within-day and between-day variability inform acceptance criteria for product qualification and contribute to monitoring instrument performance over time.
- Different instrument manufacturers utilise different terminology to express parameters such as light attenuation (and % transmission) and other settings. Reference guidance documentation and documentary standards shall be universally applicable across this range of terminology. Instrument manufacturers shall align their terminology to that recommended by international terminology standards. The community shall work together at identifying and addressing gaps in standardised terminology across the different markets.
- Instruments may differ in laser wavelength, power at both source and sample, and observed light scattering angle. These parameters affect the intensity of the scattered light that is detected and need to be optimised on a case-by-case basis. We find that the use of automatic instrument algorithms that manage the quality of the signal yields reproducible results. In general, we observed that running the instruments in automatic mode resulted in comparable settings, for example in terms of resulting light attenuation within the cuvette.
- Where this is of value, independent techniques, primarily microscopy, provide essential insights into the geometry of the particles and support interpretation of measurements performed in liquid. This is particularly important for non-spherical particles.

Overall, despite DLS being a common, fast, and user-friendly technique for the measurement of particle-based nanomedicine diameters, we have discussed some of the numerous parameters that need to be taken into account for performing robust measurements. Therefore, when reporting and capturing measurement data we encourage users to include, with the resulting Z-average and PDI values, the associated data and metadata describing sample preparation, accessories, and relevant instrument parameters. Such a comprehensive approach has the merit to enhance the understanding of nanomedicines and enable their smoother transition from development stages to the clinics – both for innovative and follow-on products.

CRediT authorship contribution statement

Ryan T. Coones: Writing – original draft, Visualization, Methodology, Investigation, Formal analysis, Data curation. **Ines Nikolic:** Writing – review & editing, Writing – original draft, Methodology, Investigation, Funding acquisition, Formal analysis, Data curation, Conceptualization. **Remo Eugster:** Writing – original draft, Methodology, Investigation, Formal analysis, Data curation. **Dora Mehn:** Writing – review & editing, Writing – original draft, Methodology, Investigation, Formal analysis, Data curation, Conceptualization. **Vivan Tong:** Writing – review & editing, Methodology, Data curation. **Paola Luciani:** Writing – review & editing, Supervision, Resources, Methodology, Investigation, Funding acquisition, Formal analysis, Data curation, Conceptualization. **Caterina Minelli:** Writing – review & editing, Writing – original draft, Supervision, Project administration, Methodology, Investigation, Funding acquisition, Formal analysis, Data curation, Conceptualization.

Declaration of competing interest

The authors declare that they have no known competing financial interests or personal relationships that could have appeared to influence the work reported in this paper.

Acknowledgement

The authors thank Valentina Petrusevska, Scott McNeill and colleagues of the NANO Working Party at the European Directorate for the Quality of Medicines and Healthcare (EDQM) for coordination of the interlaboratory study and helpful discussion of the results.

RC and CM acknowledge funding from the National Measurement Programme of the UK Department for Science, Innovation and Technology. CM has received research support from the MetrINo project. The project (22HLT04 MetrINo) has received funding from the European Partnership on Metrology, co-financed from the European Union's Horizon Europe Research and Innovation Programme and by the Participating States. CM acknowledges support from the UK Medicines and Healthcare products Regulatory Agency.

IN acknowledges funding from the Frankfurt Foundation Quality of Medicines (FFQM) through the project Quality Requirements for Nanomedicines – Filling the Gaps (grant number: 2023_02) as well as the support from the Science Fund of the Republic of Serbia through the project NanoCellEmoCog (grant number: 7749108).

DM thanks Otmar Geiss and Ivana Bianchi (Joint Research Centre) for the helpful discussions.

Cryogenic electron microscopy sample preparation and imaging were performed with devices supported by the Microscopy Imaging Centre (MIC) of the University of Bern. RE thanks Marek Kaminek and Ioan Iacovache for their support and guidance on the cryo-TEM measurements.

Appendix A. Supplementary data

Supplementary data to this article can be found online at https://doi.org/10.1016/j.ijpharm.2025.125452.

Data availability

Data will be made available on request.

References

Al-Khafaji, M.A., Gaál, A., Wacha, A., Bóta, A., Varga, Z., 2020. Materials 13, 3101.
Astier, A., Barton Pai, A., Bissig, M., Crommelin, D.J.A., Flühmann, B., Hecq, J.D., Knoeff, J., Lipp, H.P., Morell-Baladrón, A., Mühlebach, S., 2017. *Ann. N. Y. Acad. Sci.*, 1407, 50–62.
Auerbach, M., Ballard, H., 2010. Hematol. ASH Education Program. 338–347.
Bayda, S., Adeel, M., Tuccinardi, T., Cordani, M., Rizzolio, F., 2020. *Molecules* 25, 112–127.
Bloomfield, V.A., 1985. *Biological Applications*. In: Pecora, R. (Ed.), *Dynamic Light Scattering*. Spinger, New York, pp. 363–416.
Borchard, G., 2015. *Drug Nanocrystals* in D.J.A. Crommelin, D.J.A., de Vlieger, J.S.B. (Eds), *Non-Biological Complex Drugs*. Springer, pp. 171–189.
Bryant, G., Thomas, J.C., 1995. *Langmuir* 11, 2480–2485.
Bryant, G., Abeynayake, C., Thomas, J.C., 1996. *Langmuir* 12, 6224–6228.
Clogston, J.D., Hackley, V.A., Prina-Mello, A., Puri, S., Sonzini, S., Soo, P.L., 2020. *Pharm. Res.*, 37, 1–18.
Cummins, P.G., Staples, E.J., 1987. *Langmuir* 3, 1109–1113.
Di Francesco, T., Sublet, E., Borchard, G., 2019. *Eur. J. Pharm. Sci.*, 131, 69–74.
Digigow, R., Burgert, M., Luechinger, M., Sologubenko, A., Rzepiela, A.J., Handschin, S., Alston, A.E.B., Flühmann, B., Philipp, E., 2024. *Heliyon* 10, e36749.
European Commission, 2023. *Guidance on the implementation of the Commission Recommendation 2022/C 229/01 on the definition of nanomaterial*, JRC Science For policy Report.
European Medical Agency, 2016. *Guideline on the principles of regulatory acceptance of 3Rs (replacement, reduction, refinement) testing approaches*, EMA/CHMP/CVMP/JEG-3Rs/450091/2012.
European Medicine Agency, 2013. *Reflection paper on the data requirements for intravenous liposomal products developed with reference to an innovator liposomal product*, EMA/CHMP/806058/2009/Rev. 02.
European Medicines Agency, 2021. *Intravenous iron-containing medicinal products Article-31 referral - Annex I.* Annex to Assessment Report EMA/549569/2013.
European Pharmacopoeia, 2024. *Particle Size Analysis by Dynamic Light Scattering*, Ph. Eur. 2.9.50.
Farkas, N., Kramar, J.A., 2021. *J. Nanoparticle Res.*, 23, 120.
Food and Drug Administration, 2012. *Bioequivalence Recommendations for Iron Sucrose*, n. d.
Food and Drug Administration, 2013. Draft Guidance on Sodium Ferric Gluconate Complex.
Food and Drug Administration, 2024. *Draft Guidance on Ferumoxytol*.
Funk, F., Flühmann, B., Barton, A.E., 2022. Int. J. Mol. Sci. 23, 2140.
Geiss, O., Bianchi, I., El Hadri, H., Ponti, J., Brassinne, F., Wouters, C., Mast, J., Loeschner, K., Givelet, L., Cubadda, F., Raggi, A., Ferraris, F., Gräf, V., Mantovan, E. D., Zanella, M., Benetti, F., Barrero-Moreno, J., 2025. *J. Food Compos. Anal.*, 137, 1–9.
V. A. Hackley, J. D. Clogston, V. A. Hackley and J. D. And Clogston, NIST-NCL Joint Assay Protocol, PCC-1 Measuring the Size of Nanoparticles in Aqueous Media Using Batch-Mode Dynamic Light Scattering Protocol adapted from, 2010, vol. 21702.
Halamoda-Kenzaoui, B., Vandebriel, R.J., Howarth, A., Siccardi, M., David, C.A.W., Liptrott, N.J., Santin, M., Borgos, S.E., Bremer-Hoffmann, S., Caputo, F., 2021. *J. Control. Release* 336, 192–206.
Hoover, B.M., Murphy, R.M., 2020. *J. Pharm. Sci.*, 109, 452–463.
International Organization for Standardization, 2017. *Particle Size Analysis — Dynamic Light Scattering (DLS)* ISO 22412:2017.
International Organization for Standardization, 2020. *Good practice for dynamic light scattering (DLS) measurements*. ISO/TR 22814, 2020.
Kestens, V., Coleman, V.A., De Temmerman, P.J., Minelli, C., Woehlecke, H., Roebben, G., 2017. *Langmuir* 33, 8213–8224.
Kontoghiorghes, J., Chambers, S., Hoffbrand, A.V., 1987. *Biochem. J.*, 241, 87–92.
Krupnik, L., Joshi, P., Kappler, A., Flühmann, B., Alston, A.B., Digigow, R., Wick, P., Neels, A., 2023. *Eur. J. Pharm. Sci.*, 188, 106521.
Krupnik, L., Avaro, J., Liebi, M., Anaraki, N.I., Kohlbrecher, J., Sologubenko, A., Handschin, S., Rzepiela, A.J., Appel, C., Totu, T., Blanchet, C.E., Alston, A.E.B., Digigow, R., Philipp, E., Flühmann, B., Silva, B.F.B., Neels, A., Wick, P., 2024. *J. Control. Release* 368, 566–579.
Le Brun, N.E., Crow, A., Murphy, M.E.P., Mauk, A.G., Moore, G.R., 1800. *Biochim. Biophys. Acta - Gen. Subj.*, 2010, 732–744.
Li, Z., Tan, S., Li, S., Shen, Q., Wang, K., 2017. *Oncol. Rep.*, 38, 611–624.
Maguire, C.M., Rösslein, M., Wick, P., Prina-Mello, A., 2018. *Sci. Technol. Adv. Mater.*, 19, 732–745.
Mahmoudi, M., 2021. *Nat. Commun.*, 12, 1–5.
Malvern Panalytical, 2014. *Application of Dynamic Light Scattering (DLS) to Protein Therapeutic Formulations: Principles, Measurements and Analysis - 4.FAQs*. https://www.malvernpanalytical.com/en/learn/knowledge-center/whitepapers/wp140404applicdlsprotein4faq, (accessed 7 August 2024).
Martin-Malo, A., Borchard, G., Flühmann, B., Mori, C., Silverberg, D., Jankowska, E.A., Hear, E.S.C., 2019. *Fail.*, 6, 241–253.
Mühlebach, S., Flühmann, B., 2015. *Iron Carbohydrate Complexes: Characteristics and Regulatory Challenges*. In: Crommelin, D.J.A., de Vlieger, J.S.B. (Eds.), *Non-Biological Complex Drugs*. Springer, pp. 149–170.

Naiim, M., Boualem, A., Ferre, C., Jabloun, M., Jalocha, A., Ravier, P., 2015. *Soft Matter* 11, 28–32.
Nikravesh, N., Borchard, G., Hofmann, H., Philipp, E., Flühmann, B., Wick, P., 2020. Nanomed. Nanotech. Biol. Med.,, 26, 102178.
Peer, D., Karp, J.M., Hong, S., Farokhzad, O.C., Margalit, R., Langer, R., 2007. *Nat. Nanotechnol.*, 2, 751–760.
Ragheb, R., Nobbmann, U., 2020. *Sci. Rep.*, 10, 1–9.
Rottembourg, J., Kadri, A., Leonard, E., Dansaert, A., Lafuma, A., 2011. *Nephrol. Dial. Transplant* 26, 3262–3267.
Sharma, A., Beirne, J., Khamar, D., Maguire, C., Hayden, A., Hughes, H., 2023. AAPS Pharm. Sci. Tech. 24, 84.
Takahashi, K., Kramar, J.A., Farkas, N., Takahata, K., Misumi, I., Sugawara, K., Gonda, S., Ehara, K., 2019. *Metrologia* 56, 055002.
Tirado, M.M., Martinez, C.L., Garcia De La Torre, J., 1984. *J. Chem. Phys.*, 81, 2047–2052.
U.S. Pharmacopeial Convention, 2017. USP General Chapter 1225, *Validation of Compendial Procedures*.
Uhlmann, D.R., Chalmers, B., Jackson, K.A., 1964. *J. Appl. Phys.*, 35, 2986–2993.